

Article outline is loading...

JavaScript required for article outline



Safety Science

Volume 50, Issue 5, June 2012, Pages 1304–1312



A study on chest injury mechanism and the effectiveness of a headform impact test for pedestrian chest protection from vehicle collisions

Yong Han^{a, b}, , Jikuang Yang^{a, c}, Koji Mizuno^d, Yasuhiro Matsui^e^a Department of Mechanical Engineering, Xiamen University of Technology, Xiamen, China^b State Key Lab of Advanced Design and Manufacturing for Vehicle Body, Hunan University, Changsha, China^c Department of Applied Mechanics, Chalmers University of Technology, Gothenburg, Sweden^d Department of Mechanical Science and Engineering, Nagoya University, Nagoya, Japan^e National Traffic Safety and Environment Lab, Tokyo, Japan<http://dx.doi.org/10.1016/j.ssci.2011.12.002>, [How to Cite or Link Using DOI](#)[View full text](#)

Abstract

This study was aimed at investigating the injury mechanism of pedestrian chests in collisions with passenger vehicles of various frontal shapes and examining the influence of the local structural stiffness on the chest injury risk by using the headform impact test at the chest contact area of the vehicle. Three simulations of vehicle to pedestrian collisions were conducted using three validated pedestrian finite element (FE) models of three pedestrian heights of 177 (AM50th), 165 and 150 cm and three FE vehicle models representing a one-box vehicle, a minicar and a medium car. The validity of the vehicle models was evaluated by comparing the headform acceleration against the measured responses from headform impact tests. The chest impact kinematics and the injury mechanisms were analyzed in terms of the distribution of the von Mises stress of the ribcage and in terms of the chest deflections. The chest contact locations on the front panel and the bonnet top were identified in connection to the causation of rib fractures. The risk of rib fractures was predicted by using the von Mises stress distribution. The headform impact tests were carried out at the chest contact area on the front panel and bonnet to examine the safety performance with respect to pedestrian chest protection. In simulations of the one-box vehicle to pedestrian collisions, the chest was struck directly by the frontal structure at a high velocity and deformed substantially, since a shear force was generated by the stiff windshield frame. The acceleration of the headform was related to the rib deflections. The injury threshold of the ribcage deflection (42 mm) corresponded to the headform average acceleration of 68 G. In the minicar collision, the chest was struck with the bonnet top and cowl area at a low velocity, and the deformation was small due to the distributed contact force between the chest and the bonnet top. Besides, the ribcage deformation was too small for bridging a relation between the headform accelerations and rib deflections. In the medium car collision, the deformation mode of the chest was similar to that in the minicar collision. The chest collided with the bonnet top at a low velocity and deformed uniformly. The deflection of the ribs had an observable correlation with the headform accelerations measured in the headform impact tests. The frontal shape of a vehicle has a large influence on a pedestrian's chest loadings, and the chest deformation depends on the size of the pedestrian and the stiffness of the vehicle. The one-box passenger vehicle causes a high chest injury risk. The headform impactor test can be utilized for the evaluation of the local stiffness of a vehicle's frontal structure. The reduction of the headform acceleration is an effective measure for pedestrian chest protection for specific shapes of vehicles by efficacy in modifying the local structural stiffness.

Keywords

Vehicle to pedestrian collision; Chest injury; Vehicle type; Headform impact test

Figures and tables from this article:

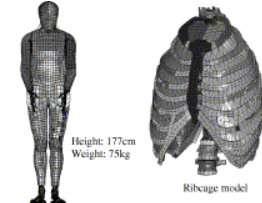


Fig. 1. The THUMS pedestrian (AM50th) and ribcage FE models.

Figure options



Fig. 2. The set up of the simulations of the vehicle and pedestrian collisions.

Figure options

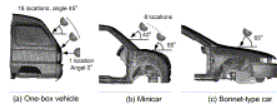


Fig. 3. The configurations of the FE simulations for the headform impacts.

Figure options

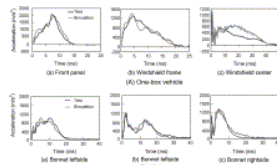


Fig. 4. The comparisons of the headform accelerations between the impact test and the FE simulation.

Figure options



Fig. 5. The kinematic behavior of the pedestrian (165 cm height) from simulations of various vehicle impacts.

Figure options

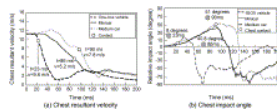


Fig. 6. The chest impact conditions (pedestrian size: 165 cm) from the simulations with different passenger vehicles.

Figure options

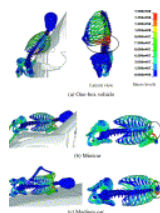


Fig. 7. The deformations of the ribcage and the von Mises stress distribution in vehicle to pedestrian (165 cm) collisions.

Figure options

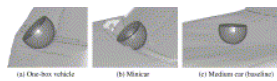


Fig. 8. The maximum deformations of the car front in the simulations of the headform impactor test.

Figure options

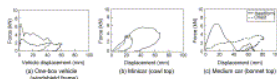


Fig. 9. The contact forces vs. the vehicle deformations in the headform impact test and in the simulations of the pedestrian chest impact (pedestrian 165 cm).

Figure options

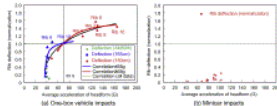


Fig. 10. The relation of the average accelerations in headform impacts and rib deformations (normalization) in pedestrian chest impacts for minicar and one-box vehicle.

Figure options

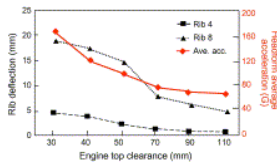


Fig. 11. The correlation between the ribs deflection and the headform average accelerations by the engine top clearance in the medium car.

Figure options

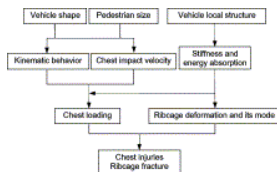


Fig. 12. The injury mechanisms of ribcage fracture.

Figure options

Table 1. Pedestrian AIS 1&2 or AIS 3+ injury region by vehicle type (ITARDA, 1999).



View Within Article

Table 2. Matrix of the FE simulations of the vehicle to pedestrian collisions.



View Within Article

Table 3. The results from FE simulation of headform impact test.



View Within Article